

1 **Temporal Variations and Source Analysis of Ambient Carbonyls in Hangzhou: A**
2 **City-Level Study in the Yangtze River Delta Region, China**

3 Haonan Xu¹, Xiaobing Pang^{1,*}, Danyun Chen¹, Zhongjian Wei¹, Yu Lu¹, Huiyi Yang^{2,3},
4 Lian Yu⁴

5
6 1. College of Environment, Zhejiang University of Technology, Hangzhou, 310014,
7 China

8 2. Natural Resources Institute, University of Greenwich, London, SE18 6NF, United
9 Kingdom

10 3. Department of Geography, University of Exeter, Exeter, EX1 2LU, United
11 Kingdom

12 4. Department of Environmental Engineering, Beijing Institute of Petrochemical
13 Technology, Beijing, 102617, China

14
15 **Abstract:** Carbonyls play an important role in the atmospheric chemistry as the main
16 precursor for reactive radicals and peroxyacetyl nitrate. However, little research has
17 been conducted so far on the seasonal variations of carbonyls in China's urban
18 atmosphere. In this study, ambient carbonyls were 24-hourly observed in four seasons
19 in Hangzhou, a mega-city in the Yangtze River Delta Region, China. The concentration
20 of total carbonyls was the highest in summer (44.35 $\mu\text{g}/\text{m}^3$), the second in winter (44.05
21 $\mu\text{g}/\text{m}^3$), the third in spring (29.31 $\mu\text{g}/\text{m}^3$) and autumn (27.11 $\mu\text{g}/\text{m}^3$). The most abundant
22 species were found to be acetone in spring, summer, and winter, while formaldehyde in
23 autumn. Rainfall can significantly reduce the concentrations of most ambient carbonyls,
24 with the largest decrease observed in the wet precipitation events occurring in spring
25 and summer, while acetone concentrations remained invariable due to its lower water
26 solubility. Multiple linear regression analysis and carbonyls ratios indicated that
27 anthropogenic emissions were the predominant sources of carbonyls, and atmospheric
28 formaldehyde was mainly emitted from primary sources other than secondary sources.
29 Vehicular exhaust was identified as the primary source of ambient carbonyls,
30 particularly in winter, and its contribution reached 92.80% to formaldehyde.
31 Additionally, photochemical reactions were closely associated with the secondary
32 production of formaldehyde in summer. Carbonyls showed strong ozone formation

33 potential in all four seasons. Based on the health risk assessment, the exposure to
34 ambient carbonyls is harmful to outdoor pedestrians. The results could provide
35 essential information and references for simulating regional air quality and analyzing
36 ozone pollution, which is essential for improving air quality in the Yangtze River Delta
37 region.

38 **Keywords:**

39 Carbonyls

40 Seasonal variations

41 Wet deposition

42 Source analysis

43 Hangzhou

44

45 -----

46 * Corresponding author

47 Dr. Xiaobing Pang.

48 E-mail: pangxb@zjut.edu.cn.

49

50 **Introduction**

51 Rapid economic development and urbanization make air quality problems more serious
52 (Ke et al., 2022). **Carbonyls are an important class of volatile organic compounds**
53 **(VOCs) characterized by carbon-oxygen double bond (C=O) structure.**
54 **Formaldehyde, acetaldehyde, and acetone are urban air's most prevalent**
55 **carbonyls. These substances are of growing concern due to their adverse effects on**
56 **human health and air quality (Zhang et al., 2019).** Carbonyls play an essential role
57 in the photochemical reactions in the atmosphere as precursors of reactive radicals
58 (RO_x), secondary organic aerosols (SOAs), and pollutants, such as peroxyacetyl nitrates
59 (PANs) and ozone (O₃) (Han et al., 2019a). It has been found that the ozone formation
60 potential (OFP) of carbonyl (166.1 μg/m³) was about 2.5 times higher than that of

61 benzene ($65.4 \mu\text{g}/\text{m}^3$) (Zhang et al., 2012). Therefore, studying the pollution
62 characteristics, source analysis, and environmental impact of carbonyls can be helpful
63 in preventing and controlling O_3 pollution, which is essential for the sustainable
64 improvement of atmospheric environmental quality.

65 **Compared to other VOCs, carbonyls exhibit higher reactivity and display**
66 **unique atmospheric behaviors. Unlike alkanes, alkenes, and aromatic**
67 **hydrocarbons, which primarily promote ozone formation through photochemical**
68 **reactions, carbonyls not only directly participate in the formation of reactive free**
69 **radicals but also influence air quality through secondary processes (Jenkin and**
70 **Clemmitshaw, 2000). Due to their relatively low atmospheric reactivity, they have**
71 **extended atmospheric lifetimes, allowing them to persist in areas distant from**
72 **their sources, thereby having a significant impact on atmospheric chemical**
73 **reactions (Mellouki et al., 2015).** Recent studies conducted in several regions of China,
74 including the Beijing-Tianjin-Hebei area, the Pearl River Delta, and focused on
75 investigating the daily variations and sources of those compounds (Wang et al., 2015;
76 Chen et al., 2014). These studies highlight the primary sources of carbonyls in urban
77 areas, including vehicle emissions, industrial activities, and incomplete combustion, as
78 well as secondary sources formed through photochemical processes. Formaldehyde,
79 acetaldehyde, and acetone are the most common carbonyl compounds found in both
80 urban and rural environments, with their concentrations typically higher, particularly in
81 urban areas, primarily due to the influence of anthropogenic sources. In particular,
82 formaldehyde plays a significant role in photochemical reactions. Under direct sunlight,
83 the photolysis of formaldehyde in the troposphere leads to the formation of HO_2 radicals,
84 which are rapidly converted into OH radicals through reactions with nitrous oxide and
85 contribute to the formation of O_3 (Garcia et al., 2006).

86 Several studies on atmospheric carbonyls have been conducted in different regions
87 to assess their impact on human health and atmospheric chemistry (Shen et al., 2021;
88 Bao et al., 2022; Franco et al., 2015; Sousa et al., 2015). However, most of them are

89 conducted for a single season, and only minimal research is on the seasonal variations
90 of atmospheric carbonyls in Chinese cities (Sun et al., 2023; Geng et al., 2022).
91 Hangzhou, the capital of Zhejiang Province, is one of the central cities in the Chinese
92 economic belt of the Yangtze River Delta, where the G20 Summit was held in 2016 and
93 the Asian Games will be held in 2023 (Li et al., 2023). With rapid economic
94 development and population growth, air pollution in Hangzhou has also been more
95 severe in recent years, with the maximum 1-hr O₃ mass concentration reaching 327
96 µg/m³ in 2016 (Han et al., 2019b). Therefore, in this study, a 24-hr observation was
97 conducted in the four seasons, combined with the meteorological data of six parameters
98 from the Hangzhou meteorological stations, to investigate the composition
99 characteristics, concentration levels, and source analysis of carbonyls in Hangzhou. The
100 health risks associated with critical species were also evaluated for Hangzhou. It aims
101 to provide essential information for regional air quality modeling studies and the source
102 apportionment of O₃ pollution, which are very important for ensuring more livable air
103 quality in the Yangtze River Delta region.

104 **1 Methodology**

105 **1.1 Sampling sites and periods**

106 As shown in **Appendix A Fig. S1**, the sampling was conducted on the campus of the
107 Zhejiang University of Technology (ZJUT, 30.30°N, 120.17°E) in Hangzhou, China,
108 located in the heart of the city and surrounded by cultural and educational areas,
109 residential areas, and major roads. The main road is 80 m from the sampling site, and a
110 tributary of the Beijing-Hangzhou Grand Canal is near the sampling area. The sampling
111 equipment is installed on the roof of a six-story school building, with the measurement
112 entrance about 25 m above the ground. Hangzhou borders the East China Sea and has
113 a typical subtropical monsoon climate. Four sampling periods were chosen for this
114 study, i.e., May 14-27, 2022 (spring), June 21-July 21, 2021 (summer), October 6-29,
115 2022 (autumn), and December 1-30, 2021 (winter).

116

117 **1.2 Carbonyls sampling and analysis**

118 The sampling and analytical procedure was based on the Environmental Protection
119 Agency (EPA) standard method TO-11 A (Huang et al., 2022). The silica gel column (a
120 Sep-Pak Silica Gel Cartridge, Waters, Millipore Corp) was thoroughly impregnated
121 with an acidified 2,4-dinitrophenylhydrazine (DNPH) solution. The solution contains
122 50 mL of acetonitrile containing 0.1 g of DNPH and orthophosphoric acid. It is then
123 blown dry with a light stream of nitrogen. The dried DNPH-coated silica gel columns
124 were sealed in PTFE bags and stored in the refrigerator at 4°C until use. Three blank
125 columns from each batch of silica gel columns were measured, all below the EPA blank
126 standard.

127 Samples of air were collected using an automated multichannel sampler developed
128 in-house. Each channel was connected to a DNPH silica gel column with a potassium
129 iodide-containing O₃ scrubber (Sep-Pak, CNW corporation, German) at the front of the
130 column to avoid interference from atmospheric O₃ (Huang et al., 2022; Shen et al.,
131 2018). The sampling was performed using a 24-hr uninterrupted experiment with a flow
132 rate of 1.0 L/min each hour from 9:00-21:00, and each 1.5 hr from 21:00-9:00. A total
133 of 20 samples could be collected daily. There was a blank sample from 9:00-21:00 and
134 a blank sample from 21:00-9:00 on each sampling day.

135 Samples and blanks were eluted slowly with the acetonitrile in 2 mL volumetric
136 flasks within 24 hr and stored in the refrigerator at 4°C for the subsequent analysis. The
137 eluted samples were passed through an HPLC-UV system (HP1100, Agilent, USA) with
138 an Acclaim 120 C18 column (5 µm, 25 cm × 4.6 mm) to determine carbonyls. The
139 chromatographic conditions were binary solvents of (A) ultrapure water and (B) pure
140 acetonitrile. The gradient elution was performed, starting with a mixture of 35% A +
141 65% B, which changed to 100% acetonitrile within 14 min. The 100% acetonitrile was
142 then changed to 35% A + 65% B within 14-16 min and held for 2 min before the next
143 sample was used (Tang et al., 2019). The injection volume was 5 µL, and the detection
144 wavelength was 360 nm.

145

146 **1.3 Quality assurance and quality control**

147 Carbonyls were characterized and quantified based on the corresponding calibration
148 standards' retention time and peak area. Six standard concentrations (0.12-1.2 mg/L)
149 were used, covering the relevant concentrations during the sampling period. There was
150 a strong linear relationship between the concentration and response of all identified
151 carbonyls, with correlation coefficients of R^2 above 0.99 for the standard curves.
152 Detailed results are shown in **Appendix A Table S1**. It should be noted that
153 tolualdehydes in this study refers to the total concentration of m-tolualdehyde and p-
154 tolualdehyde, as the analytical methods did not completely separate them. Calibration
155 standards were performed before each sample determination to ensure the instrument's
156 stability. Collection efficiency was determined using two silica columns in series, with
157 over 99% of carbonyls recovered from the first silica column and a second elution test
158 showing complete recovery of all carbonyls. The relative standard deviations of the
159 replicate analyses in this study were all less than 5%, and the method detection limit
160 (MDL) was determined by seven replicate analyses of the lowest concentration of the
161 standard. The MDL for this study ranged from 0.05 to 0.10 mg/L for a sampling volume
162 of 2 mL of the various carbonyls.

163

164 **1.4 Data analysis methods**

165 **1.4.1 Multi-linear regression model**

166 With the aim of better investigating the contribution of primary and secondary
167 sources of carbonyls, this study used a multiple linear regression model based on the
168 tracer method, using the daily concentrations of carbon monoxide (CO) and O₃ as
169 tracers and estimating the contribution of primary and secondary sources and
170 background concentrations of formaldehyde, acetaldehyde, and acetone to atmospheric
171 concentrations in four seasons by statistical analysis (Hong et al., 2018). The
172 methodological model is shown in the following equation (Lui et al., 2017):

173
$$[\text{carbonyl}] = \beta_0 + \beta_1[\text{CO}] + \beta_2[\text{O}_3] \quad (1)$$

174 where β_0 , β_1 , and β_2 (ppbv/ppbv) are coefficients determined by linear regression.
 175 $[\text{carbonyl}]$, $[\text{CO}]$, and $[\text{O}_3]$ (ppbv) are the observed volume concentrations of carbonyl,
 176 CO, and O₃. For every unit increase in CO concentration, there is a β_1 unit increase in
 177 the target carbonyl. Similarly, for each unit increase in O₃ concentration, the
 178 concentration of the target carbonyl increases by β_2 units. β_0 can be considered as the
 179 background value of the target carbonyl.

180 Therefore, the relative contributions from primary, secondary, and background
 181 sources can be calculated from the concentrations of these tracers in the environment,
 182 and the beta values can be determined using the following equations:

183
$$R_P = \frac{\beta_1[\text{CO}]_i}{\beta_0 + \beta_1[\text{CO}]_i + \beta_2[\text{O}_3]_i} \times 100\% \quad (2)$$

184
$$R_S = \frac{\beta_2[\text{O}_3]_i}{\beta_0 + \beta_1[\text{CO}]_i + \beta_2[\text{O}_3]_i} \times 100\% \quad (3)$$

185
$$R_B = \frac{\beta_0}{\beta_0 + \beta_1[\text{CO}]_i + \beta_2[\text{O}_3]_i} \times 100\% \quad (4)$$

186 Here, R_P , R_S , and R_B (%) denote the relative contribution of primary and
 187 secondary sources and background concentrations, respectively. The background
 188 concentration contribution refers to the part that cannot be explained by primary and
 189 secondary sources, such as long-range transport or carbonyls emitted by some plants.

190 **1.4.2 Ozone formation potential calculation method (OFP)**

191 OFP is an important indicator to describe the relative contribution of different
 192 VOC species to O₃ production as well as to identify the dominant species in the
 193 photochemical formation of O₃ and is applied to guide the design of O₃ mitigation
 194 measures (Li et al., 2019). OFP for individual chemical species is calculated from
 195 emission concentrations and maximum incremental reactivity (MIR), calculated as
 196 follows:

197
$$\text{OFP}_i = [\text{VOCs}]_i \times \text{MIR}_i \quad (5)$$

198 where OFP_i ($\mu\text{g}/\text{m}^3$) indicates the O₃ forming potential of VOC species i and
 199 $[\text{VOCs}]_i$ ($\mu\text{g}/\text{m}^3$) indicates the concentration of species i . MIR_i (g O₃/g VOCs) is the

200 maximum incremental response factor (MIR) for species *i*, whose specific value is
201 taken from the reference (Carter, 1994).

202 1.4.3 Health Risk Assessment

203 Health risk assessment is the estimation of the likelihood of adverse effects of a
204 hazardous substance on humans and the evaluation of the risk of human health effects
205 from exposure to that hazardous substance. In this study, the new health risk assessment
206 method (EPA-540-R-070-002) from EPA was used to quantitatively evaluate exposure
207 concentration (EC), hazard quotients (HQ), and lifetime carcinogenic risk values (Risk)
208 using the following formulas (Chaiklieng et al., 2019). The specific calculation
209 formulas are as follows:

$$210 \quad EC = \frac{C \times ET \times EF \times ED}{AT} \quad (6)$$

211 where *C* is the concentration of carbonyl measured in the environment ($\mu\text{g}/\text{m}^3$);
212 *ET* indicates the exposure time per day, indicating the outdoor exposure time, h/d; *EF*
213 indicates the exposure frequency per year, 350 d/a; *ED* indicates the lifetime exposure
214 time, a; *AT* indicates average exposure time, $AT = ED \times 365 \text{ d} \times 24 \text{ h/d}$. The average
215 exposure time in Zhejiang Province was found using the Chinese Population Exposure
216 Parameters Handbook. The average time spent outdoors in Zhejiang Province was 3.28
217 hr in both spring and autumn, 3.17 hr in summer, and 2.77 hr in winter. The average life
218 expectancy in Zhejiang Province was 77.73 years, and the *ED* was considered to be
219 77.73 years.

$$220 \quad HQ = \frac{EC}{RfC} \quad (7)$$

221 *RfC* is the guideline dose of a non-carcinogenic contaminant. The *RfC* value of
222 $9.83 \mu\text{g} \cdot \text{m}^{-3}$ was obtained from the EPA website (<http://www.epa.gov/iris>). If $HQ > 1$,
223 adverse health effects may occur; if $HQ < 1$, non-carcinogenic health effects do not
224 occur (Ehsan et al., 2020).

$$225 \quad \text{Risk} = EC \times IUR \quad (8)$$

226 The *IUR* indicates the unit intake risk or daily exposure level for carcinogens and
227 the values are also obtained from the EPA website. The *IUR* values for formaldehyde

228 and acetaldehyde are $6.0 \times 10^{-6} (\mu\text{g}/\text{m}^3)^{-1}$ and $2.7 \times 10^{-6} (\mu\text{g}/\text{m}^3)^{-1}$, respectively, and the
229 comparison of the *Risk* value with the EPA's safety threshold of 1.0×10^{-6} is used to
230 determine whether the carcinogenic risk to humans in the observed area is acceptable
231 (Qiu et al., 2018).

232

233 **2 Results and discussion**

234 **2.1 Temporal variations of carbonyls in different seasons in Hangzhou**

235 As shown in **Fig. 1**, the seasonal variation in carbonyls, conventional pollutants,
236 and associated meteorological parameters observed in Hangzhou reveals distinct
237 characteristics across different year periods. During the spring observation from May
238 14 to May 27, 2022, the average temperature was 20.93 °C, with an average wind speed
239 of 5.48 m/s. O₃ concentrations frequently exceeded the national standard, with a
240 maximum of 202 $\mu\text{g}/\text{m}^3$. **On days when O₃ concentrations exceeded the national**
241 **standard, temperatures were usually above average, while wind speeds were below**
242 **average. The results suggest that meteorological conditions such as high**
243 **temperatures, intense solar radiation, and low wind speeds are favorable for O₃**
244 **formation, as confirmed in many previous studies (Wang et al., 2001). The**
245 **observation of a significant increase in pollutants such as O₃, CO, and particulate**
246 **matter during the summer season (from June 21 to July 21, 2021), under the**
247 **influence of strong southwesterly winds, suggests a potential advection of aged and**
248 **polluted air masses into the Hangzhou metropolitan area.** At the beginning of the
249 period when photochemical pollution events were most concentrated, high CO, PM_{2.5},
250 PM₁₀, and NO₂ were accompanied by high concentrations of O₃, while carbonyls
251 remained at low levels. The reason for this is probably that photolysis of carbonyls
252 produces a primary source of free radicals, including OH and inorganic and organic
253 peroxy radicals (HO₂ and RO₂), consequently increasing photochemical O₃ production
254 (Qu et al., 2021).

255 In autumn, from October 6 to October 29, 2022, the average O₃ concentration was

256 97.04 $\mu\text{g}/\text{m}^3$, lower than in spring and summer but higher than in winter. During this
257 period, particulate matter, NO_2 , CO, and SO_2 concentrations were higher than in
258 summer, likely due to increased traffic emissions and reduced dependence on
259 photochemical reactions. The wind speed in autumn (6.49 m/s) helped to disperse
260 pollutants. Finally, during the winter observation from December 1 to December 30,
261 2021, O_3 concentrations were significantly lower, averaging 53.37 $\mu\text{g}/\text{m}^3$, with no
262 exceedances of the national standard. However, particulate matter, NO_2 , CO, and SO_2
263 concentrations were notably higher than in summer, likely due to fossil fuel combustion
264 for heating and unfavorable meteorological conditions (Deng et al., 2019; Kalogridis et
265 al., 2018). These observations indicate that seasonal changes in meteorological
266 conditions, photochemical activity, and anthropogenic emissions strongly influence
267 pollutant levels in Hangzhou.

268 From **Table 1**, nine to ten carbonyls were identified in Hangzhou across different
269 seasons, exhibiting significant seasonal variations. During the spring observation period
270 (May 14 to May 27, 2022), the average total concentration of carbonyls was 29.31
271 $\mu\text{g}/\text{m}^3$. Acetone emerged as the dominant species, with a mean concentration of 9.99
272 $\mu\text{g}/\text{m}^3$, accounting for 34.08% of the total concentration. This was followed by
273 formaldehyde and acetaldehyde, contributing 27.01% and 13.31%, respectively. **The**
274 **total carbonyl concentration, along with those of formaldehyde, acetaldehyde, and**
275 **acetone, was significantly lower in spring compared to summer and winter, likely**
276 **attributed to a combination of factors, including higher relative humidity and**
277 **lower light intensity during this period.** In the summer observation period (June 21
278 to July 21, 2021), the total carbonyl concentration rose markedly to 44.34 $\mu\text{g}/\text{m}^3$, with
279 acetone continuing to be the predominant species (19.02 $\mu\text{g}/\text{m}^3$, 42.88%).
280 Formaldehyde and acetaldehyde also displayed relatively high concentrations.
281 Compared to the other seasons, the elevated levels of carbonyls, formaldehyde, and
282 acetone in summer may be linked to high temperatures, intense solar radiation, and
283 prevailing warm southeasterly winds in the region. During autumn (October 6 to

284 October 29, 2022), the average total concentration of the ten carbonyls measured was
285 27.11 $\mu\text{g}/\text{m}^3$, with formaldehyde becoming the dominant species (6.81 $\mu\text{g}/\text{m}^3$, 25.11%),
286 followed by acetone and n-pentanal. Total carbonyl concentrations in autumn were
287 significantly lower than those in summer and winter, although n-pentanal recorded the
288 highest mean concentration. **The elevated n-pentanal concentrations observed**
289 **during the autumn may be attributed to the volatilization of n-pentane from paints**
290 **used in the renovation of a nearby building, which facilitated secondary**
291 **production of n-pentanal through photochemical reactions.** During the winter
292 observation period (December 1 to December 30, 2021), the total mean concentration
293 of carbonyls was measured at 44.04 $\mu\text{g}/\text{m}^3$, with acetone and n-butyraldehyde
294 comprising 67.31% of this total. Notably, n-butyraldehyde emerged as the second most
295 abundant compound during winter, contrasting with findings from previous studies that
296 typically identified acetone, formaldehyde, and acetaldehyde as the predominant
297 atmospheric carbonyls (Jiang et al., 2019; Wang et al., 2020; Yang et al., 2019). **The**
298 **increase in n-butyraldehyde concentration in Hangzhou during winter (10.64**
299 **$\mu\text{g}/\text{m}^3$, accounting for 24.17% of the total carbonyl compounds) may be attributed**
300 **to the increased combustion of fossil fuels for heating, with n-butane, a major**
301 **component of these fuels, being oxidized to n-butyraldehyde, along with winter**
302 **conditions that facilitate the accumulation of pollutants.** Although photochemical
303 reactions are generally less intense in winter, low wind speeds and temperature
304 inversions may facilitate the accumulation of pollutants, leading to comparable
305 carbonyl concentrations between winter and summer.

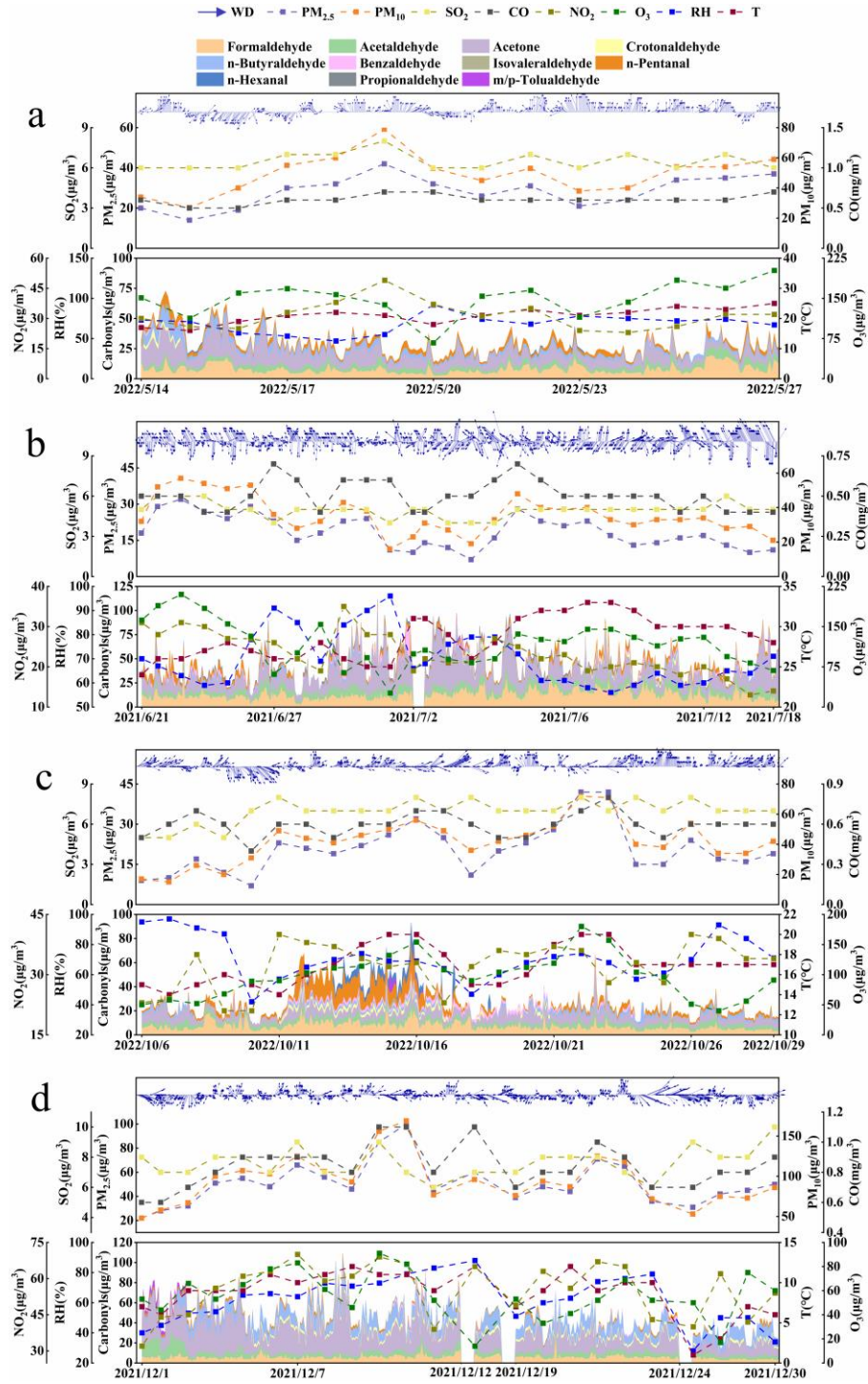
306

307

Table 1. Concentrations of carbonyls ($\mu\text{g}/\text{m}^3$) in the atmosphere of Hangzhou urban area during the observation period.

	Spring				Summer				Autumn				Winter			
	Monitoring	Proportion	Day	Night	Monitoring	Proportion	Day	Night	Monitoring	Proportion	Day	Night	Monitoring	Proportion	Day	Night
	Mean	(%)	Mean	Mean	Mean	(%)	Mean	Mean	Mean	(%)	Mean	Mean	Mean	(%)	Mean	Mean
Formaldehyde	7.92	27.01	7.85	7.98	11.73	26.45	13.19	11.29	6.81	25.11	7.13	6.49	5.29	12.01	5.70	4.88
Acetaldehyde	3.90	13.31	4.06	3.74	6.03	13.60	6.92	5.65	3.66	13.51	3.88	3.45	5.13	11.63	5.62	4.63
Acetone	9.99	34.08	12.10	7.87	19.02	42.88	22.80	16.72	6.51	24.01	7.11	5.91	19.00	43.13	21.57	16.40
Propionaldehyde	ND	ND	ND	ND	0.02	0.06	0.05	ND	ND	ND	ND	ND	ND	ND	ND	ND
Crotonaldehyde	0.18	0.61	0.26	0.10	0.38	0.85	0.34	0.46	0.78	2.88	0.87	0.69	1.79	4.06	2.03	1.55
<i>n</i> -Butyraldehyde	3.60	12.28	4.22	2.98	1.94	4.37	1.89	2.19	1.90	7.02	2.06	1.74	10.64	24.15	12.32	8.95
Benzaldehyde	0.25	0.86	0.28	0.22	1.04	2.34	1.34	0.80	1.22	4.49	1.35	1.08	0.35	0.80	0.35	0.35
Isovaleraldehyde	0.12	0.40	0.10	0.13	ND	ND	ND	ND	0.11	0.40	0.05	0.17	0.12	0.28	0.19	0.06
<i>n</i> -Pentanal	3.24	11.07	3.78	2.71	3.40	7.67	4.21	2.85	4.93	18.18	5.26	4.60	1.43	3.25	0.19	0.06
<i>m/p</i> -Tolualdehyde	ND	ND	ND	ND	0.05	0.11	0.07	0.04	0.16	0.61	0.10	0.23	0.28	0.64	1.47	1.40
<i>n</i> -Hexanal	0.11	0.38	0.05	0.18	0.74	1.67	0.82	0.72	1.03	3.79	1.05	1.00	0.02	0.05	0.03	0.01
Total	29.31	100.00	32.70	25.91	44.35	100.00	51.63	40.72	27.11	100.00	28.86	25.36	44.05	100.00	49.58	38.46

308



309

310

311

312

313

314 **2.2 Diurnal variations of carbonyls in four seasons**

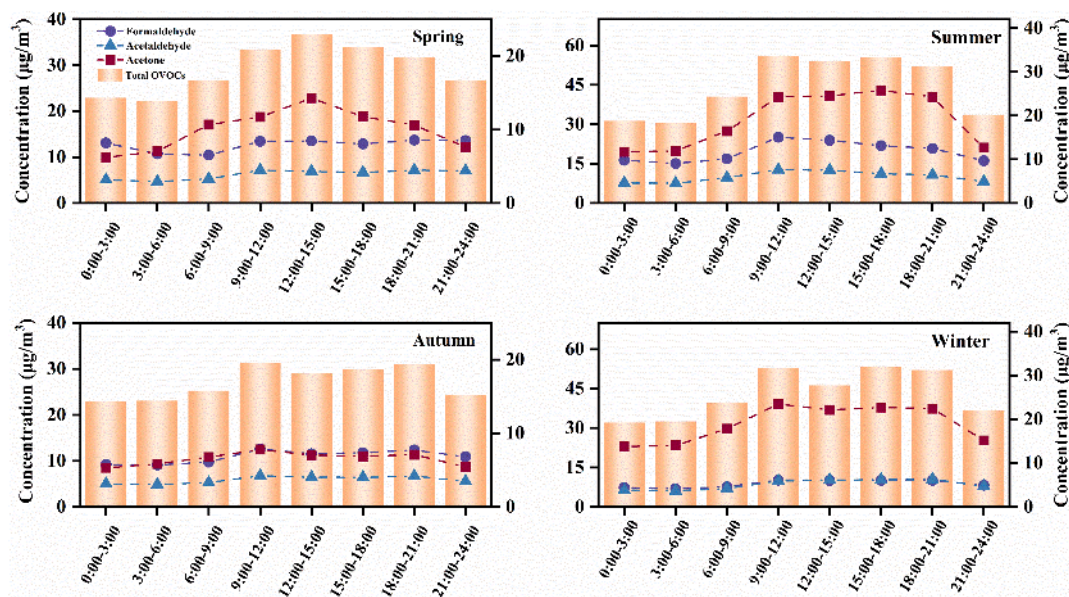
315

Fig. 2 reveals the diurnal variations of the three main compounds, formaldehyde,

316 acetaldehyde, and acetone, as well as the total carbonyls in different seasons. It can be
317 observed that the total concentration of carbonyls appears to have a clear peak in spring
318 and autumn at the same time (12:00-15:00), and this feature of the fluctuations of
319 carbonyls is mainly influenced by photochemistry (Sun et al., 2023). In contrast, two
320 relative peaks occur in summer and winter: a morning peak (9:00-12:00) and an evening
321 peak (15:00-18:00), which is similar to the morning and evening peaks abroad (Fadriani
322 et al., 2021). **Fluctuations in total carbonyl concentrations in the fall evening
323 (18:00-21:00) may be related to diurnal temperature differences, lower wind
324 speeds, and pollutant accumulation effects, in addition to precursors accumulated
325 from daytime photochemical reactions that may continue to influence
326 concentration changes during the evening hours (Feng et al., 2020).**

327 Of the four seasons, daily variations in atmospheric formaldehyde and
328 acetaldehyde concentrations were relatively uniform in winter and autumn, while
329 significant daily variations were observed in spring and summer. **Generally, the daily
330 trends of formaldehyde and acetaldehyde show a similar pattern, with
331 concentrations peaking between 9:00 and 12:00, followed by a decrease. During
332 the morning rush hour, both the number of vehicles and tailpipe emissions are
333 elevated. However, as the afternoon begins, traffic volume decreases, leading to a
334 reduction in emissions and, consequently, a decrease in the concentrations of
335 carbonyl compounds. This suggests that motor vehicle exhaust is a significant
336 anthropogenic source of pollutants in the urban area of Hangzhou. Furthermore,
337 during the midday period, increased solar radiation accelerates photolysis
338 reactions, which increases the rate at which formaldehyde and acetaldehyde are
339 broken down, leading to lower concentrations. This is consistent with the findings
340 of Guo et al. in Guangxi (Guo et al., 2016). Interestingly, a slight upward trend in
341 formaldehyde and acetaldehyde concentrations was observed at night in spring
342 and autumn, indicating a nighttime peak. This phenomenon is not coincidental.
343 During the night, temperature decreases limit vertical mixing, resulting in the**

344 accumulation of pollutants at lower altitudes. Additionally, in the absence of
 345 sunlight, photochemical reactions slow down. However, aged air masses that have
 346 already undergone photochemical reactions can transport previously formed
 347 pollutants into the region, enhancing the local accumulation of pollutants. This
 348 process likely contributes to the observed increase in formaldehyde and
 349 acetaldehyde concentrations during nighttime (Yang et al., 2017; Sun et al., 2016).



350
 351 **Fig. 2 Diurnal variations of concentrations of major carbonyls and total**
 352 **carbonyls in Hangzhou urban area in four seasons.**
 353

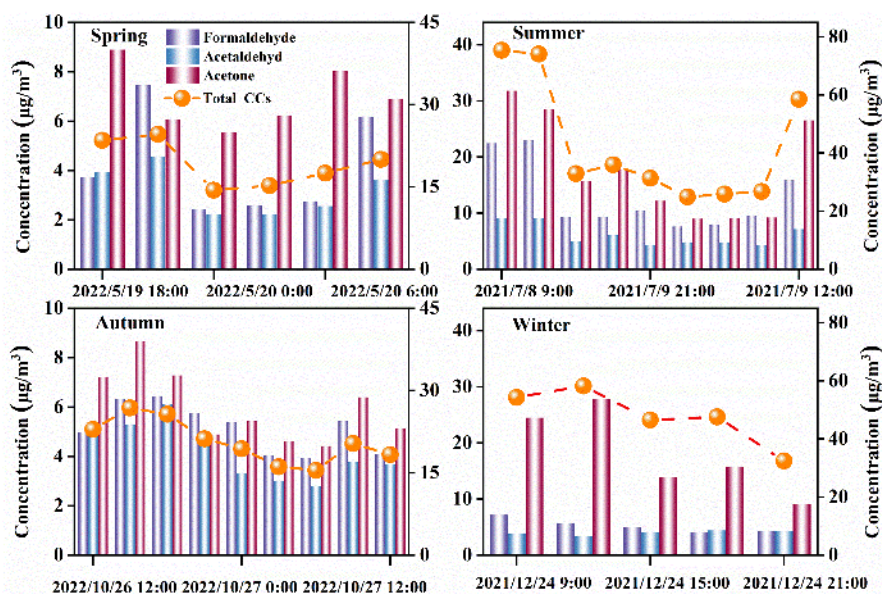
354 Compared to formaldehyde and acetaldehyde, the diurnal variations of acetone are
 355 more pronounced, with daily concentrations ranging from $5.29 \mu\text{g}/\text{m}^3$ up to $25.79 \mu\text{g}/\text{m}^3$,
 356 which is about 5 times higher. Especially in spring and autumn, acetone can reach a
 357 significant peak between 12:00 and 15:00, mainly due to photochemical secondary
 358 production. In summer and winter, on the other hand, although there is no clear peak, it
 359 is clear that the average diurnal concentrations are higher than the nocturnal ones, which
 360 is probably due to the lowering of the atmospheric boundary layer at night and the lower
 361 photochemical reactivity, resulting in much lower concentrations. **Compared to the**
 362 **spring and autumn seasons, the enhanced convection and meteorological**
 363 **instability in summer intensify the dilution and dispersion of pollutants, leading to**

364 smaller fluctuations in their concentrations. This is particularly evident in the late
365 afternoon, when strong convective activity accelerates the diffusion of pollutants,
366 making it difficult for concentrations to remain high and thus reducing the
367 likelihood of significant peaks.

368

369 2.3 Influence of Wet precipitation processes on ambient carbonyls

370 To further investigate the effects of precipitation on carbonyls concentrations, four
371 representative precipitation events in Hangzhou were selected: spring (from 18:00 to
372 11:00 on 19 May 2022), summer (from 09:00 to 11:00 on 8 July 2021), autumn (from
373 12:00 to 14:00 on 26 October 2022), and winter (from 09:00 to 24:00 on 24 December
374 2021). The analysis was conducted for four more representative precipitation processes,
375 and the changes in total and key species concentrations before and after precipitation
376 are shown in Fig. 3.



377

378 **Fig. 3 Temporal variations of carbonyls (CCs) in Hangzhou during rainfall**
379 **in different seasons.**

380

381 In spring, it started to rain in Hangzhou at around 0:00 on May 20, 2022, and it
382 rained continuously for 12 hr. The concentration of total carbonyls fluctuated in the
383 range of $14.40 \mu\text{g}/\text{m}^3 \sim 24.59 \mu\text{g}/\text{m}^3$ during the whole process, being only 58.50% of

384 the concentration before the rain, especially formaldehyde, whose concentration
385 decreased significantly at the beginning of the rain, dropping 67.16% from the
386 concentration before the rain. The total concentration of carbonyls was up to 75.39
387 $\mu\text{g}/\text{m}^3$ in the summer before the rain, and the lowest values were up to 24.88 $\mu\text{g}/\text{m}^3$
388 during the rain from about 18:00 on July 8, 2021, with the total concentration decreased
389 by 67.00%. Similar to the spring, formaldehyde concentrations decreased significantly
390 with the onset of rain, decreasing by 59.37% compared to the pre-rain period. In autumn,
391 the rain started at about 19:00 on October 26, 2022, and lasted for about 10 hr, during
392 which the total concentration of carbonyls continued to decrease, reaching 15.47 $\mu\text{g}/\text{m}^3$.
393 The concentration of carbonyls before the winter rain was 58.25 $\mu\text{g}/\text{m}^3$; from December
394 2021, precipitation started at 16:00 on December 24. It rained intermittently until 00:00
395 on December 25, when the concentration decreased sharply. The total concentration of
396 carbonyls was reduced to a minimum of 32.44 $\mu\text{g}/\text{m}^3$, which was 44.30% less than
397 before the precipitation.

398 **In general, concentrations of formaldehyde, acetaldehyde, and total**
399 **carbonyls showed a relatively stable trend during rainfall, were strongly**
400 **influenced by the reducing effect of rain, which resulted in a continuous downward**
401 **trend. In contrast, acetone concentrations exhibited more volatility.** Especially in
402 spring, acetone concentrations decreased less during rainfall. In addition, elevated
403 concentrations were observed during several precipitation events, which may be
404 attributed to the different water solubilities of the various carbonyls (Ronneau, 1987).
405 Both acetaldehyde and formaldehyde have high Henry factors and are more water
406 soluble and susceptible to rainfall than acetone (Ronneau, 1987). In addition to
407 precipitation, fog, frost, and dew, i.e., water vapor in the atmosphere, also have the same
408 effect of removing carbonyls. **Wet deposition may be one of the factors contributing**
409 **to the lower concentrations of carbonyl compounds observed at night compared**
410 **to during the day. However, other factors, such as reduced photochemical**
411 **production at night, also influence the observed nighttime concentrations.**

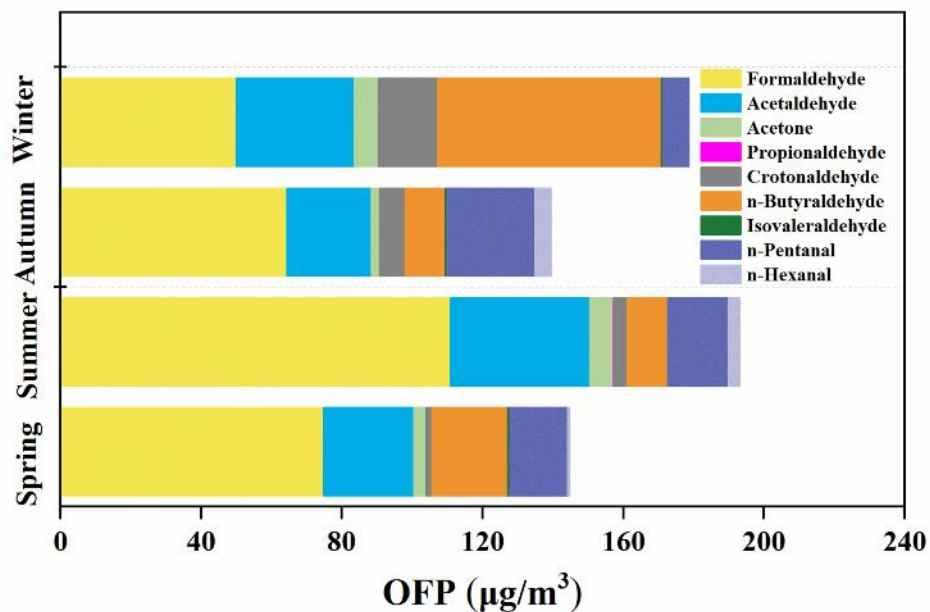
412

413 **2.4 Atmospheric environmental impact and health risk assessment**

414 **2.4.1 Ozone formation potential**

415 This study explores the potential of carbonyls to participate in photochemical
416 reactions to produce O₃ in the atmosphere of Hangzhou in four seasons. Benzaldehyde
417 and m/p-tolualdehyde were not considered in this part of the discussion due to their
418 negative MIR values and inhibitory effect on O₃ production.

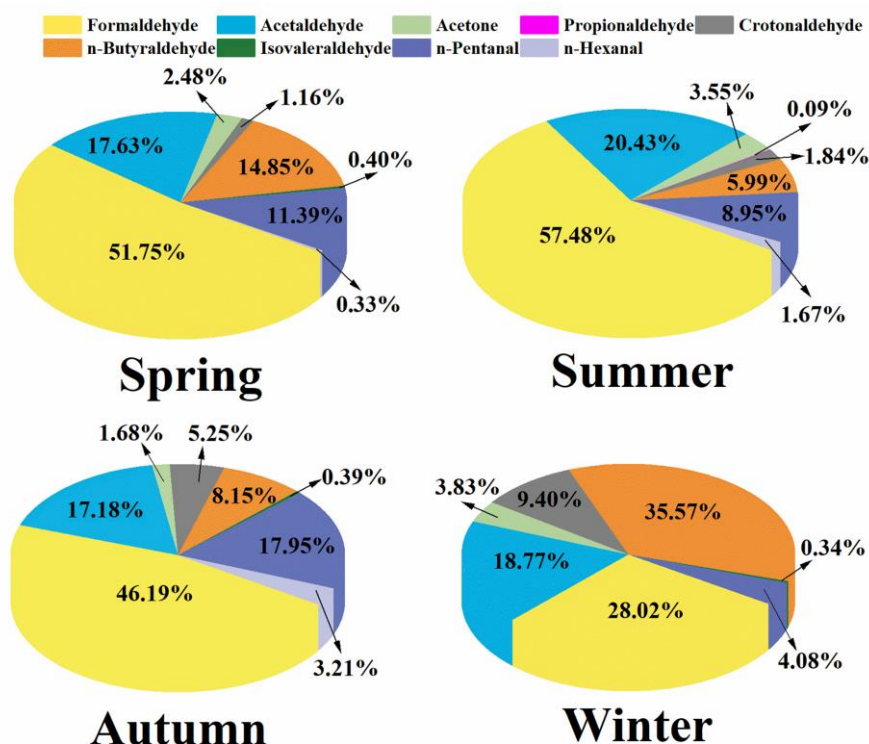
419 Here, **Fig. 4** shows the calculated results of the OFP of each carbonyl at different
420 seasons. There are apparent seasonal variations in the O₃ production from carbonyls in
421 the region for the different seasons. However, the total OFP is consistent with the
422 concentration of carbonyls in all four seasons. The contribution of carbonyls to the total
423 O₃ potential in four seasons showed that summer (193.05 μg/m³) > winter (178.66
424 μg/m³) > autumn (144.70 μg/m³) > autumn (139.42 μg/m³), which are significantly
425 higher than the observation results of other regions (Jiang et al., 2019). **Intense light in
426 summer provides favorable conditions for photochemical reactions, favoring the
427 production of OH radicals from carbonyls under solar radiation. These OH
428 radicals can then react with other pollutants, contributing to O₃ production.** Winter,
429 despite lower temperatures and weaker light, also contributes significantly to OFP due
430 to unfavorable diffusion conditions that allow the accumulation of pollutant
431 concentrations. The total OFP was close in spring and autumn and, in both cases, was
432 significantly lower than in summer and winter. A possibility exists, however, that the
433 proximity to aphelion in the autumn, with less light than in the spring, and the somewhat
434 lower pollutant concentrations during the observation period also resulted in a
435 somewhat lower total OFP than in the spring.



436
 437 **Fig. 4 Ozone formation potentials of major carbonyls in Hangzhou in four**
 438 **seasons.**
 439

440 It is further evident from **Fig. 5** that both formaldehyde and acetaldehyde in
 441 carbonyls occupy an essential position in the generation of O₃ in all seasons, with
 442 formaldehyde contributing up to 28.02%-57.48% and acetaldehyde contributing
 443 17.18%-20.43%. Aldehydes have high photochemical activity and readily react with
 444 OH radicals to form O₃, while other aldehydes contribute significantly at relatively low
 445 concentrations, such as crotonaldehyde and n-pentanal. Despite the high concentrations
 446 of carbonyls throughout the year, the contribution of acetone is low in all four seasons
 447 due to the high stability of acetone compounds, which have an MIR value of only 0.36.
 448 Therefore, the total concentrations of carbonyls are close in summer and winter, but the
 449 higher percentage of species with high MIR values in summer means that the OFP is
 450 much higher in summer than in winter. In addition, n-butyraldehyde makes a non-
 451 negligible contribution to O₃ production, especially in winter when its high
 452 concentrations cause it to surpass even formaldehyde with high MIR values as the
 453 primary contributor. Therefore, the management of pollutants can be targeted to
 454 different seasons, focusing on formaldehyde and acetaldehyde throughout the year,
 455 while in winter, focusing on n-butyraldehyde concentration can effectively reduce O₃

456 production.



457
458 **Fig. 5 Proportion of ozone formation potential of carbonyls in different**
459 **seasons in Hangzhou.**

460 **2.4.2 Health risk assessment**

461 According to the International Agency for Research on Cancer (IARC)
462 classification of carcinogens (<https://www.iarc.fr/>), acetaldehyde is classified as a Class
463 I carcinogen and formaldehyde as a Class II A carcinogen. Numerous studies prove that
464 formaldehyde and acetaldehyde are carcinogenic to humans (Zhang et al., 2019; Shen
465 et al., 2021; Bao et al., 2022). Therefore, this study selected formaldehyde and
466 acetaldehyde, which are more hazardous to human health, for health risk assessment by
467 HQ and Risk, respectively.

468 **Table 2 Health risk assessment form of formaldehyde and acetaldehyde.**

Time	Formaldehyde		Acetaldehyde	
	HQ	Risk	HQ	Risk
Spring	0.11	6.23×10^{-6}	0.05	1.38×10^{-6}

Summer	0.15	8.90×10^{-6}	0.08	2.06×10^{-6}
Autumn	0.09	5.36×10^{-6}	0.05	1.30×10^{-6}
Winter	0.06	3.51×10^{-6}	0.06	1.53×10^{-6}

469 HQ: hazard quotients; Risk: lifetime carcinogenic risk values.

470 The results are represented in **Table 2**. The non-carcinogenic risks of
471 formaldehyde and acetaldehyde are significantly different in various seasons, with HQ
472 values of 0.11, 0.15, 0.09, and 0.06 for formaldehyde and 0.05, 0.08, 0.05, and 0.06 for
473 acetaldehyde in spring, summer, autumn, and winter, respectively, during the
474 observation period, showing results well below 1. This means that the concentrations
475 of formaldehyde and acetaldehyde in the atmosphere of Hangzhou are not significant.
476 In other words, the concentrations of formaldehyde and acetaldehyde in the atmosphere
477 of Hangzhou are not significantly harmful to human health. However, it has to be noted
478 that the HQ values for both substances are significantly higher in the summer, which is
479 why it is recommended to minimize outdoor exposure in the summer. In contrast, the
480 carcinogenic risk results show that the carcinogenic risk values for the average
481 formaldehyde and acetaldehyde concentrations are higher than the international
482 maximum allowable value of 1×10^{-6} in all seasons, indicating that the atmospheric
483 concentrations of both substances in all seasons pose some carcinogenic risk to the
484 exposed population in Hangzhou and should be of concern (Qiu et al., 2018). There are
485 two effective approaches to reduce the carcinogen concentration in the area and reduce
486 the risk to humans. The first approach is to reduce the time people spend outdoors,
487 thereby reducing the risk of inhaling pollutants. Preventive and control measures can
488 be taken to further reduce the concentration of carcinogens in the environment, such as
489 wearing masks. Nevertheless, compared with the health risk assessment results of
490 formaldehyde and acetaldehyde in other cities, we can find that both the HQ and the
491 risk in Hangzhou are low. For example, the cancer risk values in Beijing, China, are
492 over 8.68×10^{-5} and in Guangzhou, China, are over 1.02×10^{-4} (Wang et al., 2014), which
493 also shows that the atmospheric environment in Hangzhou has a low cancer risk

494 compared with other observed areas.

495

496 **2.5 Formaldehyde source analysis**

497 **2.5.1 Source analysis based on carbonyls ratios**

498 Due to the similarity in sources and reaction mechanisms of carbonyls in ambient
499 air, their concentration ratios can be employed to identify contamination sources
500 preliminarily. Ratios of specific VOCs have been widely utilized for initial source
501 characterization or to gain insights into photochemical reactions. Notably, many
502 researchers now use the formaldehyde/acetaldehyde (C_1/C_2) concentration ratio as an
503 indicator for potential sources of carbonyls. This approach is based on the fact that
504 formaldehyde is primarily derived from biogenic hydrocarbons, whereas acetaldehyde
505 is predominantly produced from anthropogenic hydrocarbons. Previous studies have
506 reported that the C_1/C_2 ratio typically ranges from 1 to 2 in urban environments, while
507 in remote rural regions or areas with extensive vegetation cover, the ratio may reach
508 values as high as 10.

509 In this study, the daily averages of the C_1/C_2 ratios in Hangzhou for each season
510 were as follows: spring ranged from 1.35 to 3.35 (mean: 2.03), summer from 1.16 to
511 3.25 (mean: 1.99), fall from 1.09 to 2.74 (mean: 1.86), and winter from 0.36 to 1.49
512 (mean: 1.14). The seasonal analysis reveals that the mean C_1/C_2 ratios are similar in
513 spring and summer, with the highest mean ratio observed in summer, followed by fall,
514 and the lowest in winter. These findings are consistent with observations from other
515 cities, such as Mong Kok, Hong Kong (Cheng et al., 2014), Shenzhen (Wang et al.,
516 2017), and Rome, Italy (Possanzini et al., 1996). The elevated C_1/C_2 ratio in summer
517 can be attributed to intense solar radiation and high temperatures, which enhance
518 photochemical reactions involving VOCs. One primary loss pathway for carbonyls is
519 their reaction with OH radicals. Calculations indicate that the lifetime of C_1 when
520 reacting with OH radicals is longer than that of C_2 (Atkinson, 2000), resulting in a
521 higher C_1/C_2 ratio during summer. Conversely, during winter, photochemical reactions

522 contribute less significantly to the atmospheric concentrations of formaldehyde and
523 acetaldehyde. These results suggest that Hangzhou's primary sources of carbonyls are
524 predominantly anthropogenic.

525 Additionally, several studies have utilized the correlation between different
526 carbonyls to investigate the possibility of a common source. This study observed a
527 significant positive correlation between the mean volumetric concentrations of
528 formaldehyde and acetaldehyde, measured in samples collected simultaneously from
529 the sampling area. The Pearson correlation coefficient for this relationship was 0.42
530 ($p < 0.01$) (**Appendix A Table S2**), suggesting that the two compounds likely share
531 similar sources and atmospheric processes. **In urban areas, vehicle exhaust emissions
532 directly release large amounts of formaldehyde and acetaldehyde. Additionally,
533 VOCs released from fossil fuel combustion can undergo photochemical reactions
534 in the atmosphere to form formaldehyde and acetaldehyde. The findings of this
535 study not only support the idea of common emission sources but also emphasize
536 the potential for similar atmospheric formation pathways for these two
537 compounds.**

538 **2.5.2 Source analysis based on multiple linear regression models**

539 This study employed multiple linear regression models to quantify primary
540 emissions and secondary formation contributions to formaldehyde levels in the
541 Hangzhou urban area, using CO and O₃ as tracers for primary and secondary sources,
542 respectively. Given the high reactivity of formaldehyde, its propensity to rapidly react
543 with other atmospheric gases and compounds, and its short atmospheric lifetime,
544 background concentrations were excluded from the calculations for simplicity. **Table 3**
545 presents the regression coefficients and the contributions of primary and secondary
546 sources of formaldehyde across different seasons. The significance value (Sig) for
547 formaldehyde, within a 95% confidence interval, was 0.00, indicating the statistical
548 robustness of the model results.

549 **Table 3 Seasonal Regression Coefficients and Relative Contributions of Primary**

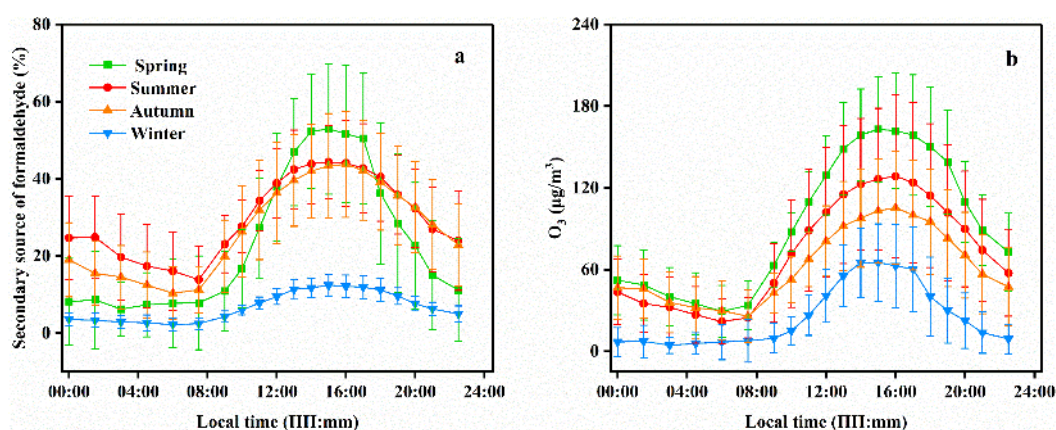
and Secondary Sources of Formaldehyde.

Season	β_0 (Background)	β_1 (Primary)	β_2 (Secondary)	Sig.
Spring	0	0.002	0.025	0.00
Relative Contributions(%)	-	74	26	
Summer	0	0.003	0.014	0.00
Relative Contributions(%)	-	69	31	
Autumn	0	0.008	0.025	0.00
Relative Contributions(%)	-	71	29	
Winter	0	0.010	0.005	0.00
Relative Contributions(%)	-	93	7	

551 Primary sources contributed more significantly to atmospheric formaldehyde
552 concentrations in Hangzhou throughout the study period than secondary sources. In
553 summer, the contribution from secondary sources of formaldehyde (30.87%) was
554 consistent with findings from Shenzhen (Wang et al., 2017) and Hong Kong (Lui et al.,
555 2017), and markedly higher than that observed in winter. The experimental results
556 demonstrated a significant positive correlation between atmospheric formaldehyde
557 concentration and temperature, with a Pearson correlation coefficient of 0.55 ($p < 0.01$),
558 while wind speed had a minimal effect, further supporting the role of photochemical
559 processes in formaldehyde formation. As a major city in China's Yangtze River Delta
560 region, Hangzhou's high volume of motor vehicles resulted in exhaust being the primary
561 source of formaldehyde emissions. **The predominance of primary sources in winter**
562 **(92.80%) suggests that direct emissions account for a large proportion of**
563 **formaldehyde sources during this season, while the contribution of photochemical**
564 **generation is relatively small.**

565 **Fig. 6** shows the daily variation in the contribution rate of secondary sources of
566 formaldehyde in Hangzhou, which exhibited a clear pattern across all seasons. The

567 contribution rate of secondary sources remained stable during nighttime, increased after
568 08:00, peaked between 15:00 and 16:00, and gradually declined. The seasonal patterns
569 of daily variation in the contribution rate of secondary sources of formaldehyde closely
570 resembled those of O₃, suggesting that secondary formaldehyde production during
571 daytime is strongly associated with photochemical reactions.



572

573 **Fig. 6 Seasonal daily variations of (a) secondary sources of formaldehyde and (b)**
574 **ozone (O₃) in Hangzhou.**

575 3 Conclusions

576 In this study, ambient carbonyls were observed in Hangzhou from 2021 to 2022.
577 The mean concentration of carbonyls in Hangzhou in spring, summer, autumn, and
578 winter were 44.35 µg/m³, 44.05 µg/m³, 9.31 µg/m³, and 27.11 µg/m³, respectively.
579 Acetone was the most abundant in spring, summer, and winter, while formaldehyde was
580 the most abundant in autumn. Rainfall can significantly reduce the concentrations of
581 formaldehyde, acetaldehyde, and total carbonyls, with the most substantial reductions
582 occurring in spring and summer. The findings indicate that wet precipitation and other
583 water vapor such as fog, frost, and dew, can effectively remove carbonyls from the
584 atmosphere, leading to lower concentrations, particularly noticeable at night. Based on
585 multiple linear regression analysis and carbonyl compound ratios, significant seasonal
586 variations were observed in the formaldehyde/acetaldehyde (C₁/C₂) concentration ratio,
587 with the highest values in summer, the lowest in winter, and intermediate values in
588 spring and autumn. These variations align with observations from other cities and are
589 related to the intensity of photochemical reactions. For example, formaldehyde in

590 Hangzhou is predominantly derived from anthropogenic sources, particularly vehicular
591 emissions, with higher contributions from secondary formation in summer and the
592 dominance of direct emissions in winter. Additionally, a significant positive correlation
593 between formaldehyde and acetaldehyde concentrations suggests they may share
594 similar sources and removal processes. The OFP results showed that the total OFP of
595 atmospheric carbonyls was consistent with their concentrations in all four seasons, with
596 summer ($193.05 \mu\text{g}/\text{m}^3$) > winter ($178.66 \mu\text{g}/\text{m}^3$) > spring ($144.70 \mu\text{g}/\text{m}^3$) > autumn
597 ($139.42 \mu\text{g}/\text{m}^3$). Based on the health risk assessment results, avoiding outdoor exposure
598 in summer is recommended.

599

600 **Acknowledgments**

601 This research work was supported by the National Natural Science Foundation of China
602 (42327806), the National Key Research and Development Program of China
603 (2022YFC3703500), the “Lead Goose” Research and Development Program of
604 Zhejiang Province (2022C03073), and the National Nature Science Foundation of
605 China (52370108).

606 **References**

- 607 1. Ke, H.B., Gong, S.L., He, J.J., Zhang, L., Cui, B., Wang, Y.Q., et al., 2022.
608 Development and application of an automated air quality forecasting system based
609 on machine learning. *Sci. Total Environ.* 806, 151204.
- 610 2. Zhang, Y.N., Xue, L.K., Dong, C., Wang, T., Mellouki, A., Zhang, Q.Z., et al., 2019.
611 Gaseous carbonyls in China's atmosphere: Tempo-spatial distributions, sources,
612 photochemical formation, and impact on air quality. *Atmos. Environ.* 214, 116863.
- 613 3. Han, Y., Huang, X.F., Wang, C., Zhu, B., He, L.Y., 2019a. Characterizing
614 oxygenated volatile organic compounds and their sources in rural atmospheres in
615 China. *J. Environ. Sci.* 81, 148-155.
- 616 4. Zhang, Y.J., Mu, Y.J., Liang, P., Xu, Z., Liu, J.F., Zhang, H.X., et al., 2012.
617 Atmospheric BTEX and carbonyls during summer seasons of 2008–2010 in

- 618 Beijing. *Atmos. Environ.* 59, 186-191.
- 619 5. Jenkin, M.E., Clemitshaw, K.C., 2000. Ozone and other secondary photochemical
620 pollutants: chemical processes governing their formation in the planetary boundary
621 layer. *Atmos. Environ.* 34 (16), 2499-2527.
- 622 6. Mellouki, A., Wallington, T.J., Chen, J., 2015. Atmospheric Chemistry of
623 Oxygenated Volatile Organic Compounds: Impacts on Air Quality and Climate.
624 *Chem. Rev.* 115 (10), 3984-4014.
- 625 7. Wang, M., Chen, W.T., Shao, M., Lu, S.H., Zeng, L.M., Hu, M., 2015. Investigation
626 of carbonyl compound sources at a rural site in the Yangtze River Delta region of
627 China. *J. Environ. Sci.* 28, 128-136.
- 628 8. Chen, W.T., Shao, M., Lu, S.H., Wang, M., Zeng, L.M., Yuan, B., et al., 2014.
629 Understanding primary and secondary sources of ambient carbonyl compounds in
630 Beijing using the PMF model. *Atmos. Chem. Phys.* 14 (6), 3047-3062.
- 631 9. Garcia, A.R., Volkamer, R., Molina, L.T., Molina, M.J., Samuelson, J., Mellqvist,
632 J., et al., 2006. Separation of emitted and photochemical formaldehyde in Mexico
633 City using a statistical analysis and a new pair of gas-phase tracers. *Atmos. Chem.*
634 *Phys.* 6 (12), 4545-4557.
- 635 10. Shen, H.Q., Liu, Y.H., Zhao, M., Li, J., Zhang, Y.N., Yang, J., et al., 2021.
636 Significance of carbonyl compounds to photochemical ozone formation in a
637 coastal city (Shantou) in eastern China. *Sci. Total Environ.* 764, 144031.
- 638 11. Bao, J.M., Li, H., Wu, Z.H., Zhang, X., Zhang, H., Li, Y.F., et al., 2022.
639 Atmospheric carbonyls in a heavy ozone pollution episode at a metropolis in
640 Southwest China: Characteristics, health risk assessment, sources analysis. *J.*
641 *Environ. Sci.* 113, 40-54.
- 642 12. Franco, C.F.J., de Mendonça Ochs, S., de Oliveira Grotz, L., de Almeida Furtado,
643 L., Pereira Netto, A.D., 2015. Simultaneous evaluation of polycyclic aromatic
644 hydrocarbons and carbonyl compounds in the atmosphere of Niterói City, RJ,
645 Brazil. *Atmos. Environ.* 106, 24-33.

- 646 13. Sousa, F.W., Cavalcante, R.M., Rocha, C.A., Nascimento, R.F., Ferreira, A.G.,
647 2015. Carbonyl compounds from urban activities and their associated cancer risks:
648 The influence of seasonality on air quality (Fortaleza-Ce, Brazil). *Urban Clim.* 13,
649 110-121.
- 650 14. Sun, J.Y., He, Y.J., Ning, Y., Xue, Z.G., Wang, H.Y., Zhang, Y.J., et al., 2023.
651 Pollution characteristics and sources of carbonyl compounds in a typical city of
652 Fenwei Plain, Linfen, in summer. *Environ. Pollut.* 320, 120913.
- 653 15. Geng, C.M., Li, S.J., Yin, B.H., Gu, C., Liu, Y.Y., Li, L.M., et al., 2022.
654 Atmospheric Carbonyl Compounds in the Central Taklimakan Desert in
655 Summertime: Ambient Levels, Composition and Sources. *Atmosphere.* 13 (5), 761.
- 656 16. Li, B.W., Ho, S.S.H., Li, X.H., Guo, L.Y., Feng, R., Fang, X.K., 2023. Pioneering
657 observation of atmospheric volatile organic compounds in Hangzhou in eastern
658 China and implications for upcoming 2022 Asian Games. *J. Environ. Sci.* 124, 723-
659 734.
- 660 17. Han, L.X., Chen, L.H., Li, K.W., Bao, Z.E., Zhao, Y.Y., Zhang, X., et al., 2019b.
661 Source Apportionment of Volatile Organic Compounds (VOCs) during Ozone
662 Polluted Days in Hangzhou, China. *Atmosphere.* 10 (12).
- 663 18. Huang, Y., Li, X.R., Chen, X., Wang, W.J., Wang, Y.H., Liu, Z.R., et al., 2022.
664 Low-molecular-weight carbonyl volatile organic compounds on the North China
665 Plain. *Atmos. Environ.* 275, 119000.
- 666 19. Shen, H.Q., Chen, Z.M., Li, H., Qian, X., Qin, X., Shi, W.X., 2018. Gas-Particle
667 Partitioning of Carbonyl Compounds in the Ambient Atmosphere. *Environ. Sci.*
668 *Technol.* 52 (19), 10997-11006.
- 669 20. Tang, G.Q., Chen, X., Li, X.R., Wang, Y.H., Yang, Y., Wang, Y.M., et al., 2019.
670 Decreased gaseous carbonyls in the North China plain from 2004 to 2017 and
671 future control measures. *Atmos. Environ.* 218, 117015.
- 672 21. Hong, Q.Q., Liu, C., Chan, K.L., Hu, Q.H., Xie, Z.Q., Liu, H.R., et al., 2018. Ship-
673 based MAX-DOAS measurements of tropospheric NO₂, SO₂, and HCHO

- 674 distribution along the Yangtze River. *Atmos. Chem. Phys.* 18 (8), 5931-5951.
- 675 22. Lui, K.H., Ho, S.S.H., Louie, P.K.K., Chan, C.S., Lee, S.C., Hu, D., et al., 2017.
676 Seasonal behavior of carbonyls and source characterization of formaldehyde
677 (HCHO) in ambient air. *Atmos. Environ.* 152, 51-60.
- 678 23. Li, M., Zhang, Q., Zheng, B., Tong, D., Lei, Y., Liu, F., et al., 2019. Persistent
679 growth of anthropogenic non-methane volatile organic compound (NMVOC)
680 emissions in China during 1990-2017: drivers, speciation and ozone formation
681 potential. *Atmos. Chem. Phys.* 19 (13), 8897-8913.
- 682 24. Carter, W.P.L., 1994. Development of Ozone Reactivity Scales for Volatile Organic
683 Compounds. *J. Air. Waste. Manage. Assoc.* 44 (7), 881-899.
- 684 25. Chaiklieng, S., Suggaravetsiri, P., Autrup, H., 2019. Risk Assessment on Benzene
685 Exposure among Gasoline Station Workers. *Int. J. Environ. Res. Public Health.* 16
686 (14), 2545.
- 687 26. Ehsan, N., Shan, A., Riaz, S., Zaman, Q.U., Javied, S., Jabeen, M., 2020. Health
688 risk assessment due to exposure of arsenic contamination in drinking water of
689 district Shiekhupura, Punjab, Pakistan. *Hum. Ecol. Risk Assess.* 26 (1), 162-176.
- 690 27. Qiu, H.L., Gui, H.R., Song, Q.X., 2018. Human health risk assessment of trace
691 elements in shallow groundwater of the Linhuan coal-mining district, Northern
692 Anhui Province, China. *Hum. Ecol. Risk Assess.* 24 (5), 1342-1351.
- 693 28. Wang, T., Wu, Y.Y., Cheung, T.F., Lam, K.S., 2001. A study of surface ozone and
694 the relation to complex wind flow in Hong Kong. *Atmos. Environ.* 35 (18), 3203-
695 3215.
- 696 29. Qu, H., Wang, Y.H., Zhang, R.X., Liu, X.X., Huey, L.G., Sjostedt, S., et al., 2021.
697 Chemical Production of Oxygenated Volatile Organic Compounds Strongly
698 Enhances Boundary-Layer Oxidation Chemistry and Ozone Production. *Environ.*
699 *Sci. Technol.* 55 (20), 13718-13727.
- 700 30. Deng, T., Wang, T.J., Wang, S.Q., Zou, Y., Yin, C.Q., Li, F., et al., 2019. Impact of
701 typhoon periphery on high ozone and high aerosol pollution in the Pearl River

- 702 Delta region. *Sci. Total Environ.* 668, 617-630.
- 703 31. Kalogridis, A.C., Vratolis, S., Liakakou, E., Gerasopoulos, E., Mihalopoulos, N.,
704 Eleftheriadis, K., 2018. Assessment of wood burning versus fossil fuel contribution
705 to wintertime black carbon and carbon monoxide concentrations in Athens, Greece.
706 *Atmos. Chem. Phys.* 18 (14), 10219-10236.
- 707 32. Jiang, Z.H., Zheng, X., Zhai, H.Q., Wang, Y.J., Wang, Q., Yang, Z.S., 2019.
708 Seasonal and diurnal characteristics of carbonyls in the urban atmosphere of
709 Changsha, a mountainous city in south-central China. *Environ. Pollut.* 253, 259-
710 267.
- 711 33. Wang, J.H., Sun, S.Y., Zhang, C.X., Xue, C.Y., Liu, P.F., Zhang, C.L., et al., 2020.
712 The pollution levels, variation characteristics, sources and implications of
713 atmospheric carbonyls in a typical rural area of North China Plain during winter. *J.*
714 *Environ. Sci.* 95, 256-265.
- 715 34. Yang, Z., Cheng, H.R., Wang, Z.W., Peng, J., Zhu, J.X., Lyu, X.P., et al., 2019.
716 Chemical characteristics of atmospheric carbonyl compounds and source
717 identification of formaldehyde in Wuhan, Central China. *Atmos. Res.* 228, 95-106.
- 718 35. Fadriani, H., Hidayat, I., Adinda, N.R., Haris, S., Mahardika, A.G., Nuryono, B.,
719 2021. Analysis of Unsignalized Intersection Using PKJI 2014 Method (Study Case:
720 Intersection of Jalan Sukajadi - Jalan Sukawangi-Jalan Sindang Sirna, Bandung).
721 *J. Phys.: Conf. Ser.* 1764 (1), 012160.
- 722 36. Feng, X., Wei, S., Wang, S., 2020. Temperature inversions in the atmospheric
723 boundary layer and lower troposphere over the Sichuan Basin, China: Climatology
724 and impacts on air pollution. *Sci. Total Environ.* 726, 138579.
- 725 37. Guo, S.J., Chen, M., Tan, J.H., 2016. Seasonal and diurnal characteristics of
726 atmospheric carbonyls in Nanning, China. *Atmos. Res.* 169, 46-53.
- 727 38. Yang, X.Q., Xue, L.K., Yao, L., Yao, L., Li, Q.Y., Wen, L., et al., 2017. Carbonyl
728 compounds at Mount Tai in the North China Plain: Characteristics, sources, and
729 effects on ozone formation. *Atmos. Res.* 196, 53-61.

- 730 39. Sun, L., Xue, L.K., Wang, T., Gao, J., Ding, A.J., Cooper, O.R., et al., 2016.
731 Significant increase of summertime ozone at Mount Tai in Central Eastern China.
732 *Atmos. Chem. Phys.* 16 (16), 10637-10650.
- 733 40. Ronneau, C., 1987. *Atmospheric Chemistry: Fundamentals and Experimental*
734 *Techniques*, Eos, Transactions American Geophysical Union. John Wiley & Sons,
735 Ltd, pp. 1643-1643.
- 736 41. Wang, B.G., Xia, L., Zhou, L., Wang, H., Zhang, C.L., 2014. A Health Risk
737 Assessment of Carbonyl-containing Volatile Organic Compounds in the
738 Atmosphere of Chinese Megacities. *Soc. Sci. China.* 35 (3), 143-157.
- 739 42. Cheng, Y., Lee, S.C., Huang, Y., Ho, K.F., Ho, S.S.H., Yau, P.S., et al., 2014.
740 Diurnal and seasonal trends of carbonyl compounds in roadside, urban, and
741 suburban environment of Hong Kong. *Atmos. Environ.* 89, 43-51.
- 742 43. Wang, C., Huang, X.F., Han, Y., Zhu, B., He, L.Y., 2017. Sources and Potential
743 Photochemical Roles of Formaldehyde in an Urban Atmosphere in South China. *J.*
744 *Geophys. Res.-Atmos.* 122 (21), 11934-11947.
- 745 44. Possanzini, M., Di Palo, V., Petricca, M., Fratarcangeli, R., Brocco, D., 1996.
746 Measurements of lower carbonyls in Rome ambient air. *Atmos. Environ.* 30 (22),
747 3757-3764.
- 748 45. Atkinson, R., 2000. Atmospheric chemistry of VOCs and NO_x. *Atmos. Environ.*
749 34 (12), 2063-2101.
- 750